

Article

# Development of Highly Efficient Hydroisodeparaffinization Catalysts Based on Micro-Mesoporous SAPO-31: New Approaches in the Synthesis of SAPO-31 and the Preparation of Bifunctional Catalysts

Gennady V. Echevsky \*, Aleksander V. Toktarev, Evgeny G. Kodenev and Dmitry G. Aksenov

Boriskov Institute of Catalysis SB RAS, 630090 Novosibirsk, Russia; atok@catalysis.ru (A.V.T.); egv@academ.org (E.G.K.)

\* Correspondence: egv@catalysis.ru

**Abstract:** A method is proposed for the synthesis of micro-mesoporous SAPO-31 with a high external surface area and large mesopore volume using tetraethoxysilane as a source of silicon. The synthesis of SAPO-31 is based on the principles underlying the Stöber process approach, which allows control of the pore diameter and volume and, hence, the external surface area of the product material. The use of the proposed methods for depositing the hydro-dehydrogenating component on the synthesized micro-mesoporous SAPO-31 made it possible to obtain highly efficient bifunctional hydroisodeparaffinization catalysts with the platinum or palladium content not higher than 0.2 wt.%. As a result, the process temperature can be decreased by 50–60 °C in comparison with the known analogs. Therewith, for example, in the test reaction of n-decane hydroisodeparaffinization at a temperature of 300 °C and feed rate of 1.5 h<sup>-1</sup>, the conversion above 90%, and the 97–98% yield of liquid products, the 95% selectivity to isomeric products were achieved.

**Keywords:** SAPO-31; silicoalumophosphate; Stöber process; tetraethoxysilane; micro-mesoporous materials; bifunctional hydroisodeparaffinization catalysts



**Citation:** Echevsky, G.V.; Toktarev, A.V.; Kodenev, E.G.; Aksenov, D.G. Development of Highly Efficient Hydroisodeparaffinization Catalysts Based on Micro-Mesoporous SAPO-31: New Approaches in the Synthesis of SAPO-31 and the Preparation of Bifunctional Catalysts. *Catalysts* **2023**, *13*, 810. <https://doi.org/10.3390/catal13050810>

Academic Editor: Wladimir Reschetilowski

Received: 27 February 2023

Revised: 21 April 2023

Accepted: 22 April 2023

Published: 27 April 2023



**Copyright:** © 2023 by the authors. Licensee MDPI, Basel, Switzerland. This article is an open access article distributed under the terms and conditions of the Creative Commons Attribution (CC BY) license (<https://creativecommons.org/licenses/by/4.0/>).

## 1. Introduction

In the conventional technique used to prepare a mixture for the hydrothermal synthesis of SAPO-31 silicoalumophosphate, a source of silicon is introduced into the mixture in the second step after mixing phosphoric acid with a source of aluminum (pseudoboehmite), i.e., before introducing a template into the mixture [1,2]. Such an order of steps is usually justified by the fact that at pH values 1.5–2.5 after the first step the particles of the disperse SiO<sub>2</sub> phase in water possess a low coagulation rate. Moreover, if tetraethoxysilane serves as a source of SiO<sub>2</sub>, it is essential also that the hydrolysis rate of tetraethoxysilane in an acid medium is much higher than at nearly neutral pH values. However, the literature provides no examples of the stable synthesis of phase-pure SAPO-31 having a micro-mesoporous structure and high crystallinity.

To obtain silica (SiO<sub>2</sub>) in the form of particles of uniform size [3–5], the Stöber process is used—a chemical process used in materials science. Werner Stöber and his team reported this in 1968 [3]. This is an example of a sol–gel process in which the molecular precursor is usually tetraethylorthosilicate. As a result of the reaction, silica particles with a diameter of less than 2000 nm are formed depending on the conditions. This process has been investigated since the time of its discovery; attempts were made to understand its kinetics and mechanism. Raman spectroscopy was used to study the NH<sub>3</sub>-catalyzed formation of colloidal silica particles from TEOS in methanol and ethanol. The growth of silica particles was found to have an incubation period, after which the essential nucleation does not occur [6]. The particles have a homogeneous structure and low polydispersity.

Silica produced by the Stöber process is the perfect material to be used as a model for investigation of colloidal phenomena [7] due to monodispersity (homogeneity) of its particle sizes [8]. The Stöber materials made of porous silica are applied in catalysis [9] and liquid chromatography due to their high surface area and a homogeneous, tunable and highly ordered pore structure.

The Stöber process is a sol-gel approach to the production of monodisperse silica ( $\text{SiO}_2$ ). The materials obtained by the Stöber process are still widely used.

The one-step Stöber process (Figure 1):

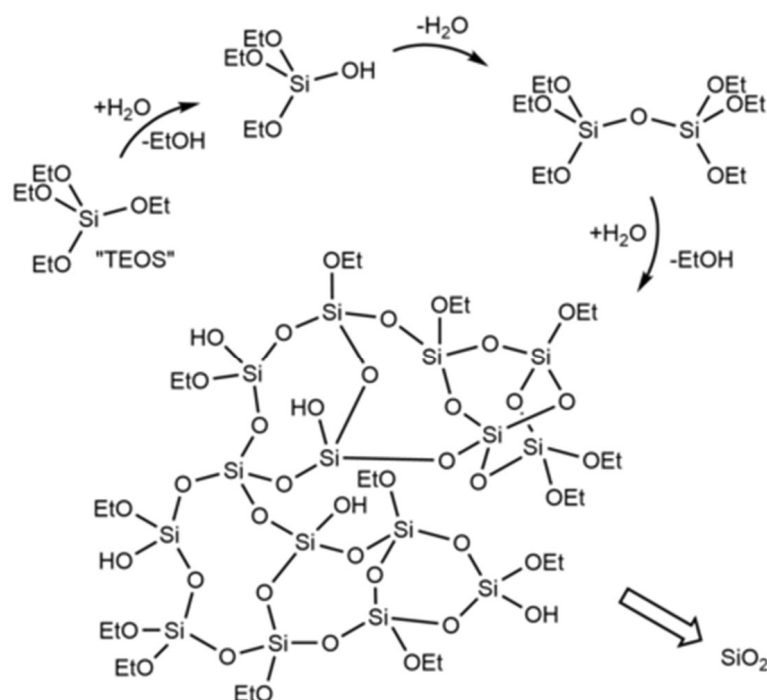
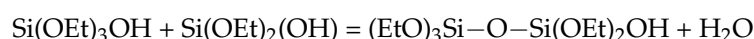
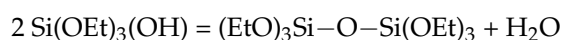


**Figure 1.** A simplified scheme of hydrolysis and condensation of TEOS in the Stöber process.

The reaction yields ethanol and a mixture of ethoxysilanols (such as  $\text{Si}(\text{OEt})_3\text{OH}$ ,  $\text{Si}(\text{OEt})_2(\text{OH})_2$ , and even  $\text{Si}(\text{OH})_4$ ):



A mixture of ethoxysilanols can then condense with either TEOS or another silanol with the loss of alcohol or water [10]

Further hydrolysis of ethoxy groups and subsequent condensation lead to the formation of cross-links.

The process produces particles of colloidal silica with a diameter of 50 to 2000 nm, the distribution of which is determined by the concentration of reagents, catalysts and temperature. The concentration of TEOS is inversely proportional to the size of the particles formed due to the greater number of nucleation centers. The process depends on temperature, and cooling leads to an increase in particle size.

The one-step Stöber process can be modified for the production of porous silica by introducing a template (a surfactant) into the reaction mixture and calcination of the obtained particles [11].

The pore volume and surface area of the product material can be controlled by varying the surfactant concentration [12].

The one-step Stöber process for the production of porous silica, which was modified by adding a template (a surfactant) to the reaction mixture before introducing a source of silicon, can give the following results. The surfactant forms small micelles with the hydrophobic internal part and the hydrophilic surface; a silicoalumophosphate–silica network grows around the micelles to form particles with the channels filled with the surfactant [11].

All over the world, silicoaluminophosphate with the AEL (SAPO-11) structure is mainly used for the preparation of hydroisodeparaffinization catalysts [13]. At the same time, this is not the only structure among silicoaluminophosphates that is successfully used for the hydroisodeparaffinization of n-paraffins. According to data from the literature [14,15], SAPO-31 silicoaluminophosphate (ATO) is a one-dimensional porous structure with a diameter of inlet windows ( $0.54 \times 0.54$  nm) and has comparable activity and selectivity in the conversion of n-alkanes.

Insufficient attention to SAPO-31 silicoalumophosphates is caused to a great extent by the absence of simple and reliable methods for their synthesis; therewith, physicochemical and catalytic properties of the materials belonging to this structural type have not been properly studied.

The following goals were specified in our study:

- a. To develop an innovative method for the synthesis of phase-pure SAPO-31 with a micro-mesoporous structure based on tetraethylorthosilicate as a source of silicon using approaches of the modified Stöber process;
- b. To create a highly efficient bifunctional hydroisodeparaffinization catalyst based on the synthesized SAPO-31.

## 2. Results and Discussion

Our earlier study [16] revealed that if sources of silicon have a different nature (silica sol, methakaolin), the properties of the synthesized samples differ and strongly depend on conditions and the duration of the silicon source dissolution (depolymerization). This is related to different particle morphology of the initial compound (spherical particles with a size of 30–40 nm in the case of silica sol or very thin nanoplates in the case of methakaolin). Different morphology and size of the silicon source particles lead to different degrees of their depolymerization in the dissolution step and, accordingly, to different degrees of silicon involvement in constructing the crystalline framework.

The following conclusions can be made from the optimization of conditions for the synthesis of microporous materials with the structural type ATO (SAPO-31) using different silicon sources to obtain SAPO-31 with the maximum crystallinity. When pseudoboehmite was used as a source of aluminum and dibutylamine (DBA) served as a template, the synthesis of silicoalumophosphate samples with the SAPO-31 structure using different sources of silicon led to the formation of SAPO-31 with different morphology and crystallinity. The use of different silicon sources improved physicochemical properties of the synthesized silicoalumophosphate powders in the series:

Silica sol < methakaolin < tetraethoxysilane.

The scanning electron microscopy data displayed in Figure 2 show that the amount of foreign phases (“garbage”) and the thickness of single-crystal plates in polycrystallites decrease when moving from silica sol to methakaolin and then to tetraethoxysilane as a source of silicon.

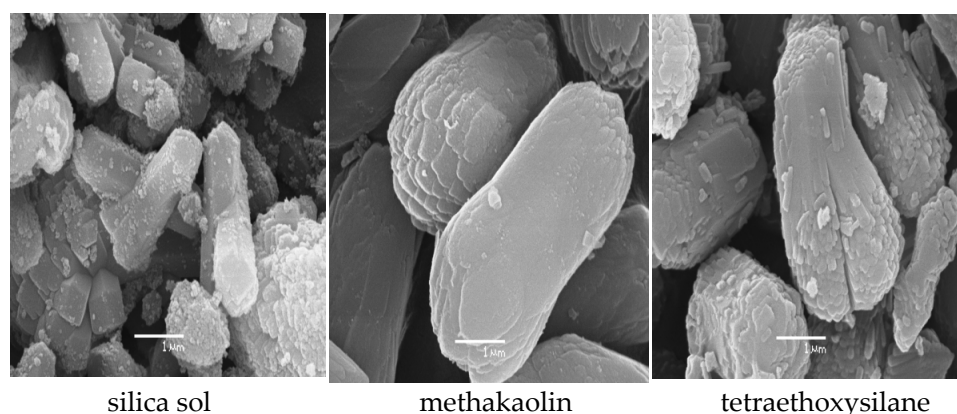


**Figure 2.** Microimages of SAPO-31 samples synthesized using different sources of silicon.

Furthermore, we studied the synthesis of SAPO-31 using TEOS as a source of silicon, which allowed reaching the maximum dispersion of the silicon source. Therewith, we introduced the reagents in an order that differed from the conventional one. Namely, in the second step a secondary amine was added, while TEOS was added in the third step. The procedures of introducing both the amine and the source of  $\text{SiO}_2$  did not differ from the conventional method of mixture preparation. The only distinction was the time of homogenizing the mixture after the addition of reagents. Thus, after adding the amine, the mixture was mixed only for 30 min (instead of 2 h), assuming that the amine would not react completely and the remaining part would serve as a catalyst for the hydrolysis of tetraethoxysilane (the modified Stöber process). Accordingly, the mixing time after the introduction of tetraethoxysilane into the mixture was extended from 1 to 2 h.

Figures 3 and 4 display the diffraction patterns of the SAPO-31 samples synthesized with the conventional order of mixing the reagents (Figure 3) and with the order changed according to the modified Stöber process (Figure 4).

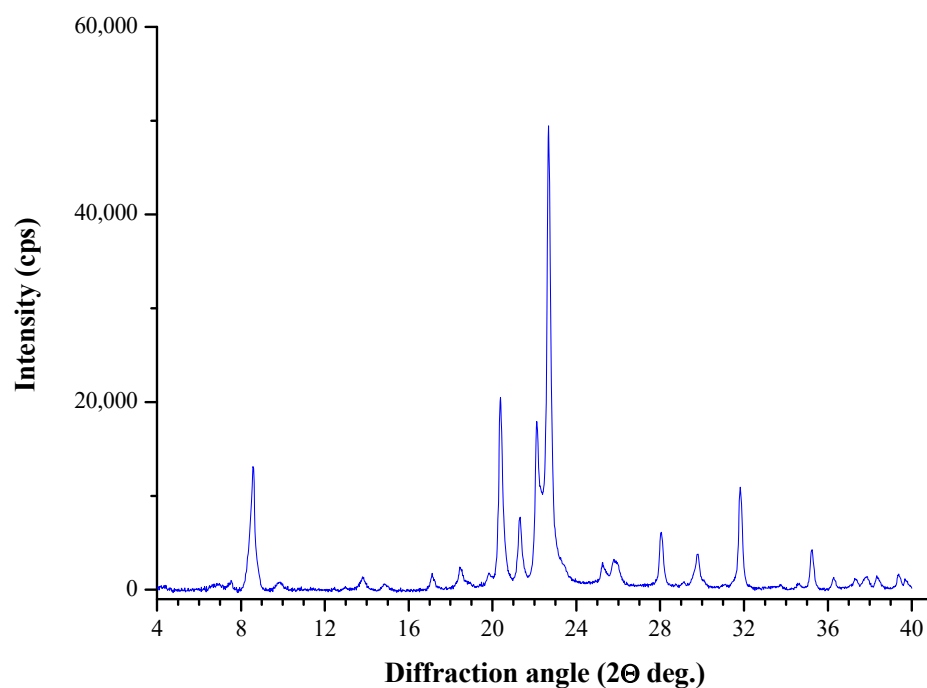


**Figure 3.** Diffraction pattern of the SAPO-31 sample with the conventional order of mixing the reagents.

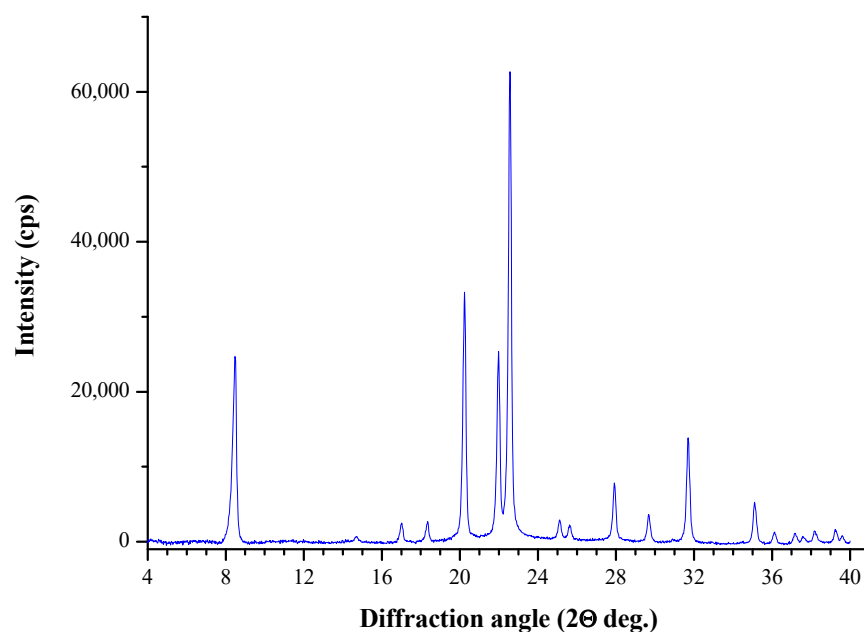


**Figure 4.** Diffraction pattern of the SAPO-31 sample with the changed order of mixing the reagents (the modified Stöber process).

It is seen that the use of the modified Stöber process in the preparation of a mixture for the synthesis leads to the formation of the phase-pure product.

It is known from the literature [17] that the surface of colloidal silicic acid particles has a positive charge up to the isoelectric point, which is caused by the sorption of  $H^+$  cations. A decrease in the negative charge on the surface of silicic acid particles at  $pH > 5$  results from coagulation of the sol. It is known that coagulation of sols can proceed by the concentration or neutralization mechanism. Neutralization–coagulation occurs upon the addition of non-indifferent electrolyte to the sol. In this process, the potential determining ions are bound to form a poorly soluble compound.

Table 1 lists the results of the SAPO-31 synthesis using TEOS as a silicon source with the conventional order of preparing a mixture for the synthesis and with the use of the modified Stöber process. DBA and DPA served as the templates.

**Table 1.** The yield of SAPO-31 (ATO) and SAPO-11 (AEL) structures in dependence on the pH of the initial mixture.

Sample	pH Ini	pH Fin	% ATO	% AEL
ATO-1 (DBA)	5.7	7.91	81	19
ATO-2 * (DBA)	6.7	7.75	32	68
ATO-3 (DBA)	5.7	7.51	84	16
ATO-4 (DPA)	6.3	7.27	34	66
ATO-4 ** (DPA)	5.5	7.51	>95	<5

\*—the conventional order of preparing a mixture for the synthesis. \*\*—ATO-4\*\* was prepared by the same procedure as ATO-4; however, after the second step (the introduction of amine), the pH of the mixture was additionally corrected to decrease it from 6.3 to 5.5 by adding concentrated phosphoric acid.

Figure 5 displays diffraction patterns of the corresponding samples. According to Table 1 and Figure 5, the maximum yield of the SAPO-31 phase is observed when the pH of the initial mixture before the synthesis is  $\leq 5.5$  (i.e., in the region of isoelectric point). To obtain the maximum yield of the desired structure (SAPO-31), samples were further synthesized, if necessary, at the pH value corrected to  $\leq 5.5$  after introducing the template (the modified Stöber process).

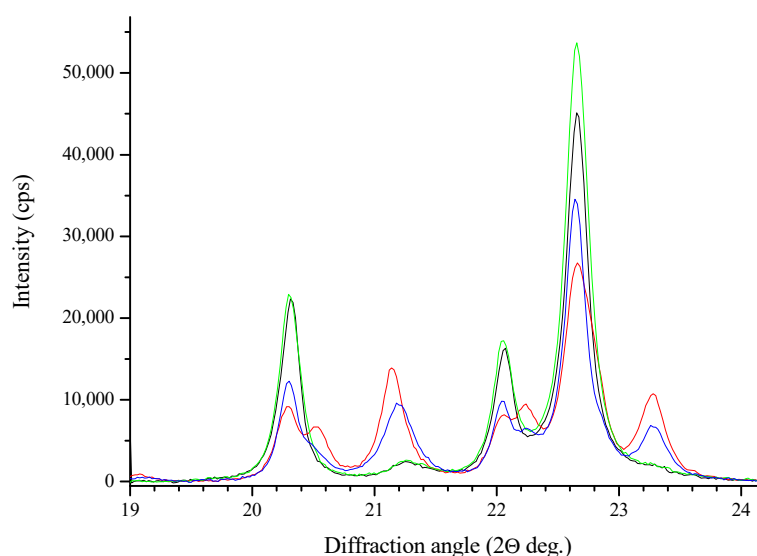


**Figure 5.** XRD patterns of ATO-1 (black line), ATO-2 (red line), ATO-3 (green line) and ATO-4 (blue line) samples.

The approach described above was applied to synthesize samples with differing silicon content. The data obtained by the investigation of their structural characteristics are listed in Table 2.

**Table 2.** Structural characteristics (surface area and pore volume) of the SAPO-31 samples with differing silicon content, which were synthesized using TEOS as a source of silicon within the modified Stöber process approach.

Samples	Surface Area (m <sup>2</sup> /g)			Pore Volume (cm <sup>3</sup> /g)		
	BET	Micropores	External	Total	Micropores	Mesopores
SAPO-31-T-0.1 *	215	190	25	0.090	0.075	0.015
SAPO-31-T-0.05	224	186	38	0.117	0.062	0.055
SAPO-31-T-0.1	200	145	56	0.144	0.056	0.088
SAPO-31-T-0.2	222	120	102	0.219	0.045	0.174

\*—the conventional order of preparing a mixture for the synthesis.

Relative amounts of BAS in the synthesized samples were estimated from the area of the signal in the IR spectrum at a frequency of 1545 cm<sup>-1</sup>. The results listed in Table 3 show that an increase in the silicon content leads to a growth in the amount of acid sites, predominantly the strong ones.

**Table 3.** Concentration of Brønsted acid sites in SAPO-31 with differing silicon content, which were synthesized with the use of TEOS.

Samples	Concentration of Brønsted Acid Sites, μmol/g			
	Total	Weak	Moderate	Strong
SAPO-31-T-0.1 *	86	32	26	28
SAPO-31-T-0.05	98	37	25	36
SAPO-31-T-0.1	145	40	37	68
SAPO-31-T-0.2	171	45	41	85

\*—the conventional order of preparing a mixture for the synthesis.

Thus, the results obtained demonstrate that application of the modified Stöber process approach makes it possible to sustainably synthesize the phase-pure micro-mesoporous

SAPO-31 using TEOS as a source of silicon and DBA or DPA as templates. Therewith, the number of moderate and strong acid sites in the synthesized samples in case of the modified Stöber process approach increases as compared to the conventional order of preparing a mixture for the synthesis.

According to the theory of polyfunctional catalysis [18], the activity and selectivity of bifunctional catalysts, particularly in the hydrotreatment of hydrocarbons, are determined by the ratio of acidic and hydrogenating functions of the catalyst (without regard to molecular sieve effects). In our case, the hydrogenating function is determined by palladium, while the acidic one is by SAPO-31.

The hydrogenating function is determined by the following factors:

- Specific hydrogenating activity of the metallic component (in our case it is constant);
- Surface area of the metallic component (the dispersion degree);
- Distribution over a silicoalumophosphate crystal.

To reveal the effect exerted by the deposition temperature on the dispersion of palladium (and its distribution), the bifunctional catalysts modified with palladium were synthesized using the same SAPO-31-T-0.2 support at 25, 70 and 85 °C. The results are listed in Table 4. The dispersion degree of the metal increases with increasing of the deposition temperature.

**Table 4.** Dispersion degree of metallic palladium in the Pd/SAPO-31 catalysts synthesized with the use of TEOS.

Samples	Dispersion of Metal, % of Theoretical Value
0.2%Pd/SAPO-31-T-0.2-I-25 °C	16.7
0.2%Pd/SAPO-31-T-0.2-I-70 °C	59.5
0.2%Pd/SAPO-31-T-0.2-I-85 °C	68.4

Figures 6 and 7 show the yield and formation selectivity of C<sub>10</sub> isomers versus the reaction temperature over the bifunctional catalysts based on SAPO-31, which were synthesized using either the conventional order of preparing a mixture for the synthesis (TEOS, DBA) or the modified Stöber process approach (DBA, TEOS).

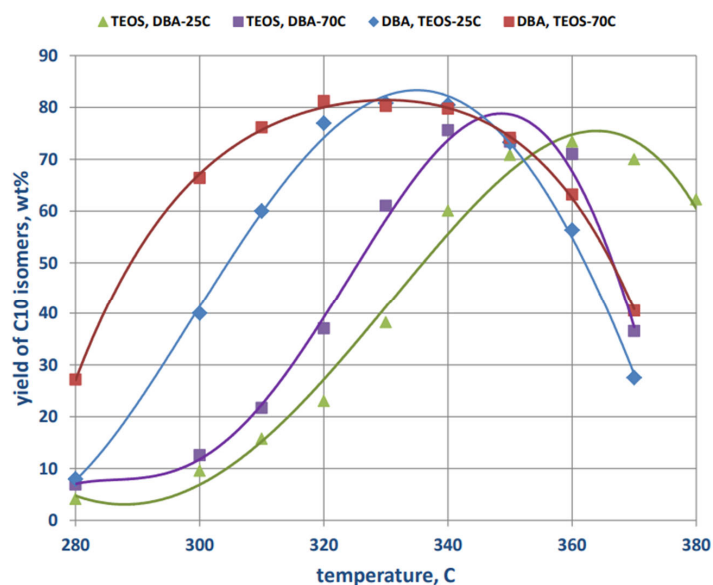


**Figure 6.** The yield of C<sub>10</sub> isomers in dependence on the reaction temperature over bifunctional catalysts at different palladium deposition temperatures.

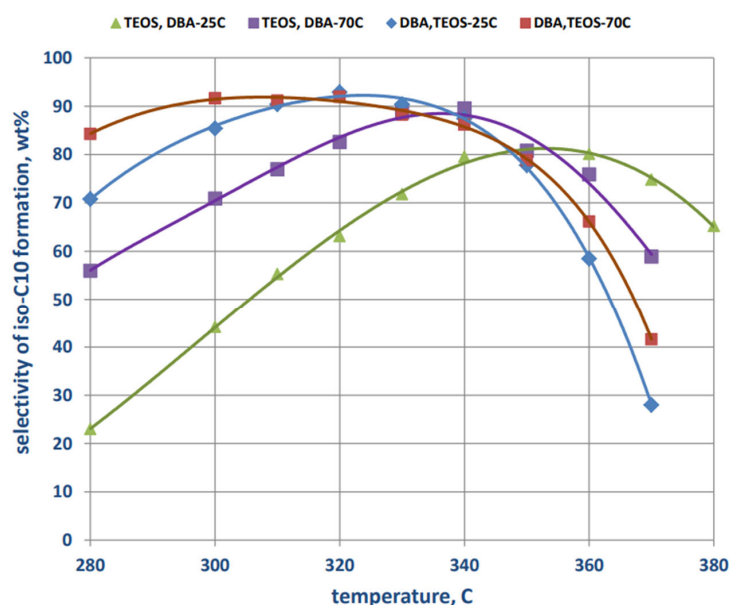


**Figure 7.** The formation selectivity of C<sub>10</sub> isomers in dependence on the reaction temperature over bifunctional catalysts at different palladium deposition temperatures.

The experiments revealed that, first, the palladium deposition temperature of 85 °C is not practically feasible to some extent, and second, the dispersion of the produced palladium is excessive because it decreases the formation selectivity of isomers due to enhancing the hydrogenolysis reaction.

When the palladium deposition temperature is varied from 25 to 70 °C, the activity of the bifunctional catalyst increases in both variants of preparing a mixture for the synthesis. However, the synthesis within the modified Stöber process approach makes it possible to obtain the most efficient bifunctional catalyst. The temperature of n-decane hydroisomerization can be decreased by 50–60 °C without changes in the yield of isomers and selectivity of their formation.

### 3. Materials and Methods

#### 3.1. Preparation of Microporous Materials with the ATO Structural Type

The following reagents were employed in the study:

- (1) Phosphoric acid, pure, GOST 6552-80, 85.1 wt.% H<sub>3</sub>PO<sub>4</sub>;
- (2) Pseudoboehmite, AlOOH, Catapal B (Sasol, the Republic of South Africa), 76.8% Al<sub>2</sub>O<sub>3</sub>;
- (3) Di-n-butylamine (DBA), HNBU<sub>2</sub>, (99%, Aldrich);
- (4) Dipropylamine (DPA) (99%, Aldrich);
- (5) Silica sol, Ludox LS30 (DuPont, USA), 30 wt.% SiO<sub>2</sub>, 0.21 wt.% Na<sub>2</sub>O;
- (6) Methakaolin ( $\omega_{\text{SiO}_2} = 54.8\%$ ,  $\omega_{\text{Al}_2\text{O}_3} = 42.1\%$ );
- (7) Tetraethoxysilane, Si(OC<sub>2</sub>H<sub>5</sub>)<sub>4</sub>, (98%, Aldrich);
- (8) Distilled water;
- (9) Palladium(II) chloride (59% Pd), anhydrous, Merck 8.07110.8500;
- (10) n-Decane (99%, Reakhim).

Microporous materials within the ATO structure were synthesized by hydrothermal treatment of the reaction gel, which was prepared by mixing the initial reagents in certain ratios: the sources of aluminum, phosphorus, silicon and the template compound.

Silicoalumophosphates were obtained in several series of experiments with the variation of some parameters of the mixture preparation. In the general form, the composition of the initial mixture had the following molar ratios of components:





where  $\text{Al}_2\text{O}_3$  is the source of aluminum,  $\text{P}_2\text{O}_5$ —the source of phosphorus,  $\text{SiO}_2$ —the source of silicon, and DBA—the template (DBA). Parameter  $x$  could take the following values: 0.05, 0.1, 0.2 and 0.3.

The initial mixture was prepared by mixing on an IKARW 16 mechanical instrument using a propeller mixer.

### 3.2. The Basic Preparation Procedure of the Reaction Mixture for the Synthesis

In our experiments, the basic procedure for preparing the reaction mixture used the conventional order of mixing the reagents. The calculated amount of phosphoric acid was diluted with a part of the calculated water amount. Pseudoboehmite was placed in a vessel with a phosphoric acid solution and mixed by an impeller mixer for 2 h.

In the next step, according to the conventional preparation technique, the mixture was supplemented with a source of silicon [1]. The presence of this step is related to the low coagulation rate of the particles of the disperse  $\text{SiO}_2$  phase at the pH values (1.5–2.5) formed in the first step. In addition, in the case of tetraethoxysilane as a source of  $\text{SiO}_2$ , it is essential also that the hydrolysis rate of tetraethoxysilane in an acid medium is much higher than at nearly neutral pH values.

In the third step, a secondary amine was added to the reaction mixture. After the introduction of the entire calculated amount of the amine, the reaction mixture was mixed during 2 h.

In the final step, SAPO-31 seed crystals were added to the reaction mixture. The seed powder was preliminarily ground in a porcelain mortar for 10 min. Upon introduction of the seed crystals, the mixture was mixed for 10 min, the pH was measured, and the mixture in a teflon insert was placed in an autoclave.

After the hydrothermal synthesis under static conditions (temperature 180 °C, 48 h), the autoclave was cooled in cold running water for 30 min, opened, and the pH of the mixture was measured.

The synthesized SAPO-31 was activated in a PM-8 muffle furnace under static conditions (without air feeding) for further deposition of the hydrogenating component (Pd). To this end, a sample in a quartz cup was placed in a cold muffle cabinet, and programmed heating was switched on. Temperature control and adjustment were performed using a temperature controller Thermodat-14E5. Calcination was carried out by the following program: heating at a temperature ramp rate of 100°/h from room temperature to 200 °C; holding at 200 °C for 2 h; a temperature rise from 200 to 380 °C at a rate of 100°/h; holding at 380 °C for 2.5 h; a temperature rise from 380 to 500 °C at a rate of 100°/h; holding at 500 °C for 3 h; a temperature rise from 500 to 600 °C at a rate of 240°/h; holding at 600 °C for 4 h; switching off the heating; and cooling of the muffle cabinet.

Metal-containing silicoalumophosphates SAPO-31 with the metal content in the range of 0.2–0.5 wt.% were prepared by the impregnation coupled with ion exchange in the temperature range from 20 to 85 °C.

X-ray diffraction analysis (XRD) was conducted using a high resolution diffractometer HZG-4C (Carl Zeiss, Oberkochen, Germany) in an angular range of  $2\theta = 4\text{--}40^\circ$  (a  $\text{CuK}_\alpha$  source). Crystallinity of materials of the ATO structural type was estimated from reflection areas in the range of  $2\theta$  diffraction angles from 19 to 24°. To this end, a sample with the highest crystallinity was chosen as the reference one. Crystallinity was estimated within an error of  $\pm 5\%$ .

Scanning electron microscopy on Leo 1430 (Carl Zeiss, Oberkochen, Germany) and Hitachi S-4800 (Ibaraki, Japan) was used to determine the morphology of the resulting crystalline materials. The BET method and the t-plot method were used to calculate the specific surface area and pore volume of nitrogen-adsorption isotherms in the pressure range  $p/p_0$  between 10<sup>−6</sup> and 0.995 on the Autosorb-1-C/TCD instrument (Cantachrome Instruments, Boynton Beach, USA). It also determined the dispersion of the deposited metal by the chemisorption of hydrogen. The chemical composition was determined by X-ray fluorescence spectroscopy.

For separate determination of Brønsted (BAS) and Lewis (LAS) acid sites in the synthesized samples, IR spectroscopy of adsorbed pyridine (Py-IRS) was also employed. These experiments were carried out using a PES Spectrum 100 IR Fourier spectrometer equipped with a high-temperature cell with CaF<sub>2</sub> windows. Samples of silicoalumophosphates were pressed into pellets with a surface density of 0.009–0.014 g/cm<sup>2</sup>, placed in a cell, and purged in a flow of high-purity helium at a pressure of  $1.33 \times 10^{-2}$  Pa and a temperature increased up to 350 °C at a rate of 5°/min. At this temperature the samples were purged for two hours and then cooled to room temperature. The adsorption of pyridine was performed at room temperature by injecting a portion of purified pyridine with an injector into the gas line through a special port. After the pyridine injection, the sample under consideration was purged in a helium flow at 150 °C for 30 min, after which the temperature was reduced to room values, and the IR spectrum was recorded. Relative amounts of BAS and LAS in the synthesized samples were estimated from the areas of the corresponding signals in the IR spectrum over the frequency range of 1400–1600 cm<sup>-1</sup> using  $\epsilon$ -molar extinction coefficients for the bands of pyridine adsorbed on BAS and LAS, which were taken from ref. [19].

The catalytic properties of palladium-modified microporous materials with the ATO structural type were investigated on a catalytic flow setup using a steel fixed-bed reactor (the catalyst loading of 7 g (10 mL) and the 0.4–0.8 mm grain size). The experiments were carried out over the temperature range of 280–340 °C at a pressure  $P = 3.0$  MPa, weight hourly space velocity of n-decane (WHSV) = 1.5–2 h<sup>-1</sup>, and hydrogen space velocity 590 h<sup>-1</sup>. n-Decane served as the initial feedstock in the study. Before the experiments, the catalyst was activated in the reactor in flowing hydrogen at 250 or 400 °C and the reaction pressure for an hour. After leaving the reactor, the conversion products were cooled in a refrigerator–separator. The reaction products were analyzed with an Agilent-6850 chromatograph using a flame-ionization detector and a capillary chromatographic column HP-1 with subsequent computer processing of the obtained results.

#### 4. Conclusions

The synthesis of SAPO-31 with TEOS as a source of silicon was carried out using the Stöber process approach, which allows controlling the mesopore diameter and volume and, hence, the external surface area of the product material. Thus, it is possible to synthesize the micro-mesoporous silicoalumophosphate SAPO-31 having high crystallinity, small crystal size, and a high external surface area. The proposed methods of depositing the hydro-dehydrogenating component on the synthesized micro-mesoporous SAPO-31 can be applied to obtain highly efficient bifunctional hydroisodeparaffinization catalysts with the palladium content not higher than 0.2 wt.%. The process temperature can be decreased by 50–60 °C in comparison with the known analogs. Therewith, for example, the test reaction of n-decane hydroisodeparaffinization at a temperature of 300 °C and feed rate of 1.5 h<sup>-1</sup> provides the conversion above 90%, the 97–98% yield of liquid products, and the 95% selectivity of isomeric products.

**Author Contributions:** G.V.E.—Conceptualization, methodology, data curation, writing—original draft preparation, writing—review and editing; A.V.T.—formal analysis, investigation, visualization; E.G.K.—investigation, visualization; D.G.A.—investigation, visualization. All authors have read and agreed to the published version of the manuscript.

**Funding:** This work was conducted within the framework of budget project No. 0239-2021-0014 for Boreskov Institute of Catalysis.

**Conflicts of Interest:** The authors declare no conflict of interest.

## References

1. Lok, B.M.; Messina, C.A.; Patton, R.L.; Gajek, R.T.; Cannan, T.R.; Flanigen, E.M. Crystalline Silicoaluminophosphates. U.S. Patent 4440871, 3 April 1984.
2. Miller, S.J. Methods for Preparing Substantially Pure SAPO-31 Silicoaluminophosphate Molecular Sieve. U.S. Patent 5230881, 27 July 1993.
3. Stöber, W.; Fink, A.; Bohn, E. Controlled growth of monodisperse silica spheres in the micron size range. *J. Colloid Interface Sci.* **1968**, *26*, 62–69. [[CrossRef](#)]
4. Bogush, G.H.; Tracy, M.A.; Zukoski, C.F. Preparation of monodisperse silica particles: Control of size and mass fraction. *J. Non-Cryst. Solids* **1988**, *104*, 95–106. [[CrossRef](#)]
5. Kicklebick, G. Nanoparticles and Composites. In *The Sol-Gel Handbook: Synthesis, Characterization and Applications*; Wiley: Hoboken, NJ, USA, 2015; Volume 3, pp. 227–244.
6. Matsoukas, T.; Gulari, E. Dynamics of growth of silica particles from ammonia-catalyzed hydrolysis of tetra-ethyl-orthosilicate. *J. Colloid Interface Sci.* **1988**, *124*, 252–261. [[CrossRef](#)]
7. Berg, J.C. (Ed.) *An Introduction to Interfaces and Colloids: The Bridge to Nanoscience*; World Scientific Publishing Co. Pte. Ltd.: Singapore, 2009.
8. Boday, D.J.; Wertz, J.T.; Kuczynski, J.P. *Functionalization of Silica Nanoparticles for Corrosion Prevention of Underlying Metal*; Kong, E.S.W., Ed.; Wiley: Hoboken, NJ, USA, 2015.
9. Giraldo, L.F.; López, B.L.; Pérez, L.; Urrego, S.; Sierra, L.; Mes, M. *Mesoporous Silica Applications*; Wiley: Hoboken, NJ, USA, 2007; Volume 258.
10. Van Blaaderen, A.; Van Geest, J.; Vrij, A. Monodisperse Colloidal Silica Spheres from Tetraalkoxysilanes: Particle Formation and Growth Mechanism. *J. Colloid Interface Sci.* **1992**, *154*, 481–501. [[CrossRef](#)]
11. Grün, M.; Lauer, I.; Unger, K.K. The synthesis of micrometer- and submicrometer-size spheres of ordered mesoporous oxide MCM-41. *Adv. Mater.* **1997**, *9*, 254–257. [[CrossRef](#)]
12. Liu, S.; Lu, L.; Yang, Z.; Cool, P.; Vansant, E.F. Further investigations on the modified Stöber method for spherical MCM-41. *Mater. Chem. Phys.* **2006**, *97*, 203–206. [[CrossRef](#)]
13. Guo, L.; Fan, Y.; Bao, X.; Shi, G.; Liu, H. Two-stage surfactant-assisted crystallization for enhancing SAPO-11 acidity to improve n-octane di-branched isomerization. *J. Catal.* **2013**, *301*, 162–173. [[CrossRef](#)]
14. Mériaudeau, P.; Tuan, V.A.; Nghiem, V.T.; Lai, S.Y.; Hung, L.N.; Naccache, C. SAPO-11, SAPO-31 and SAPO-41 molecular sieves: Synthesis, characterization and catalytic properties in n-octane hydroisomerization. *J. Catal.* **1997**, *169*, 55–66. [[CrossRef](#)]
15. Sinha, A.K.; Seelan, S. Characterization of SAPO-11 and SAPO-31 synthesized from aqueous and non-aqueous media. *Appl. Catal. A Gen.* **2004**, *270*, 245–252. [[CrossRef](#)]
16. Echevsky, G.V.; Toktarev, A.V.; Qi, W.; Wei, W. Effect of the type of silicon source on the physicochemical and catalytic properties of mesoporous silicoaluminophosphate molecular sieves. *Pet. Chem.* **2016**, *56*, 244–252. [[CrossRef](#)]
17. Smirnova, M.Y.; Kikhtyanin, O.V.; Rumyantseva, E.L. Sol-gel processes during decomposition of highly basic slag with acid. *Young Sci.* **2013**, *7*, 27–30.
18. Weisz, P.B. Polyfunctional Heterogeneous Catalysis. *Adv. Catal.* **1962**, *13*, 137–190.
19. Smirnova, M.Y.; Kalinkin, A.V.; Titkov, A.I.; Ayupov, A.B.; Ermakov, D.Y. Effect of calcination temperature on the properties of Pt/SAPO-31 catalyst in one-stage transformation of sunflower oil to green diesel. *Appl. Catal. A* **2015**, *505*, 524–531. [[CrossRef](#)]

**Disclaimer/Publisher’s Note:** The statements, opinions and data contained in all publications are solely those of the individual author(s) and contributor(s) and not of MDPI and/or the editor(s). MDPI and/or the editor(s) disclaim responsibility for any injury to people or property resulting from any ideas, methods, instructions or products referred to in the content.